

# SOFT X-RAY AR<sup>+8</sup> LASERS AND WAKE-FIELD ELECTRON ACCELERATORS BY USING LOW-CURRENT CAPILLARY Z-PINCHES

B. Fekete<sup>1</sup>, M. Kiss<sup>1</sup>, A. A. Shapolov<sup>1</sup>, S. Szatmari<sup>2</sup>, S.V. Kukhlevsky<sup>1</sup>

<sup>1</sup>*Institute of Physics, University of Pecs, Ifjusag u. 6, 7624 Pecs, Hungary*

<sup>2</sup>*Institute of Experimental Physics, University of Szeged, Dom Ter 9, 6720 Szeged, Hungary*

DOI: <https://doi.org/10.14232/kvantumelektronika.9.7>

## 1. Introduction

The soft X-ray (46.9 nm) Ar<sup>+8</sup> lasers based on capillary discharge Z-pinch plasmas require the excitation pulses with short (a few hundred ns) periods and high (a few tens kA-s) amplitudes. Such pulses are usually produced by high-voltage (up to ~ 800 kV) Marx generators in a C-C charge-transfer scheme. The Ar<sup>+8</sup> lasers can operate by using the capillary Z-pinch pulses with lower amplitude ( $I \sim 10$  kA) and shorter ( $T/2 \sim 100$  ns) current half-periods produced, for instance, by an impulse transformer driven by a high-voltage Marx-generator. Our goal is the development of compact soft X-ray lasers excited by the low current ( $I_{\min} < 10$  kA) and low charge-voltage ( $U < 100$  kV) pumping systems [1, 2]. Our MHD simulations, which are based on a one-fluid, two-temperature, one-dimensional magneto-hydrodynamic model [3, 4] of capillary Z-pinch discharges and atomic kinetic code, showed that the low current and low charge-voltage could be sufficient for the achievement of the mirror-less lasing. One of our pumping systems (transformerless system), does use a double Z-pinch directly produced by the Marx-generator in the three-electrode longitudinal discharge (double capillary channel). Another pumping scheme is based on the use of an impulse transformer without using the high-voltage Marx generator for the transformer primer circuit. The present study describes preliminary results of the theoretical analysis, development, and experimental investigation of these two pumping schemes. Properties of the laser-plasma channels have been analyzed by using our MHD simulations based on the aforementioned one-fluid, two-temperature, and one-dimensional magneto-hydrodynamic model and atomic kinetic code for different parameters of the pumping scheme.

The investigation of wake-field acceleration of electrons by laser pulse in plasma waveguides produced by capillary Z-pinch has been conducted in [5, 6]. In this paper, we present a theoretical investigation of the wake-field acceleration of electrons by CO<sub>2</sub>-laser pulse with a wavelength of 10.6 $\mu$ m and input peak intensity of  $>10^{15}$  W/cm<sup>2</sup> in transient hydrogen-plasma waveguide produced by the capillary Z-pinch.

## 2. Atomic kinetic code and magnetohydrodynamic model

Refraction-reduced (effective) laser gain is given by

$$G_{eff} = \frac{\lambda^4}{8\pi\Delta\lambda} A_{ul} \left( n_{iu}^Z - n_{il}^Z \frac{g_u}{g_l} \right) - \frac{F_{cyl}}{r} \sqrt{\frac{n_e}{n_e^c}}, \quad (1)$$

where  $A_{ul}$  is the radiation decay rate,  $g_{u/l}$  is the statistical weight of the upper/lower energy level,  $F_{cyl}$  is the geometrical factor and  $n_e^c$  is the critical electron density. Balance equations of the ion energy levels read

$$\frac{dn_{ik}^Z}{dt} = \sum_{m>k} n_{im}^Z [n_e (C_{km}^{ex} - C_{mk}^{de}) + A_{mk}] - n_{ik}^Z \sum_{m<k} [n_e (C_{mk}^{ex} + C_{km}^{de}) + E(\tau_{km}) A_{km}], \quad (2)$$

where  $C_{km}^{ex}$  and  $C_{mk}^{dx}$  are the excitation and de-excitation coefficients. The simplified formula of escape factor  $E(\tau_{km})$  at  $\tau_{km}$  optical depth is given by

$$E = 1 - \pi^{-1} \int_{-X}^X e^{-x^2} (1 - \exp[-\tau_{km} \exp[-x^2]]) dx. \quad (3)$$

The plasma parameters for the atomic kinetic code were calculated by using the magneto-hydrodynamic equations (4-9):

$$\frac{\partial n_i}{\partial t} + \frac{1}{r} \frac{\partial}{\partial r} (rv_r n_i)_i = 0, \quad (4)$$

$$m_i n_i \left( \frac{\partial v_r}{\partial t} + v_r \frac{\partial v_r}{\partial r} \right) = J_z \frac{\partial A_z}{\partial r} - \frac{\partial p}{\partial r} - \frac{1}{r} \frac{\partial}{\partial r} (r\pi_{rr}) + \frac{\pi_{\varphi\varphi}}{r}, \quad (5)$$

$$\frac{3}{2} n_e \left( \frac{\partial T_e}{\partial t} + v_r \frac{\partial T_e}{\partial r} \right) = -\frac{p_r}{r} \frac{\partial}{\partial r} (rv_r) - \frac{1}{r} \frac{\partial}{\partial r} (rq_e^r) - \pi_e^{rr} \frac{\partial v_r}{\partial r} - \pi_e^{r\varphi} \frac{v_r}{r} - \pi_e^{rz} \frac{\partial v_r^{ez}}{\partial r} + Q_e, \quad (6)$$

$$\frac{3}{2} n_i \left( \frac{\partial T_i}{\partial t} + v_r \frac{\partial T_i}{\partial r} \right) = -\frac{p_i}{r} \frac{\partial}{\partial r} (rv_r) - \frac{1}{r} \frac{\partial}{\partial r} (rq_i^r) - \pi_i^{rr} \frac{\partial v_r}{\partial r} - \pi_i^{r\varphi} \frac{v_r}{r} + Q_i, \quad (7)$$

$$\frac{1}{r} \frac{\partial}{\partial r} (rA_z) = \mu_0 A_z, \quad (8)$$

$$\frac{\partial J_z}{\partial t} + \frac{1}{r} \frac{\partial}{\partial r} (rv_r J_z) = \frac{e}{m_e} \frac{\partial}{\partial r} (r\pi_z^r), \quad (9)$$

where  $n_e$  and  $n_i$  are the electron and ion densities,  $v_r$  is the plasma radial velocity,  $J_z$  is the axial current density,  $A_z$  is the axial vector potential,  $p$  is the plasma pressure,  $\pi_{\alpha\beta}$  is the stress tensor,  $q_i^r$  and  $q_e^r$  are the radial ion and electron a heat flows,  $Q_i$  and  $Q_e$  are the heating power densities of ions and electrons.

### 3. Soft X-ray Ar<sup>+8</sup> laser by capillary, low-current, double Z-pinch

In the argon-filled capillary, the soft x-ray ( $\lambda = 46.9$  nm) Ar<sup>+8</sup> lasers excited by the two-electrode Z-pinch discharge with the short (a few hundred ns) periods and high (a few ten kA-s) amplitudes have been investigated in the last years. In the present study, the soft x-ray Ar<sup>+8</sup> laser pumped by the three-electrode Z-pinch discharge in the double capillary channel was modeled and experimentally investigated.

The experimental set-up, laser scheme, and diagnostics are shown in Figs. 1. The six-stage Marx generator ( $C_0 \sim 5$  nF) produces  $\sim 200$  kV output voltage. The water dielectric capacitor ( $C_1 = 4.4$  nF) is connected to the Marx generator through the inductance coil ( $L \sim 6\mu$ H). The two Ar<sup>+8</sup>-plasma channels were generated inside the 3 mm-inner-diameter alumina capillary during the discharge of  $C_1$  switched by the water spark gap (SG).

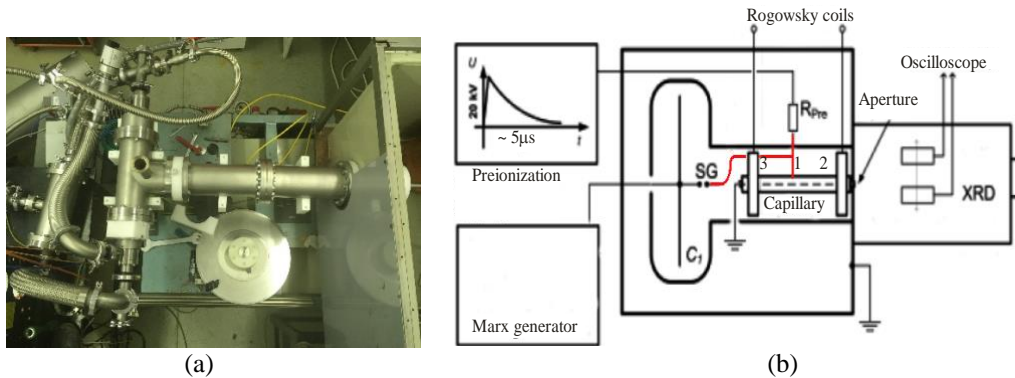
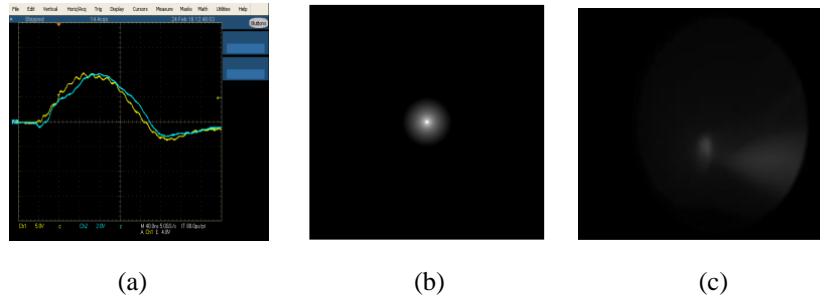


Fig.1

Photo (a) and scheme (b) of the laser experimental set-up and diagnostics of Ar<sup>+8</sup> laser.

The pumping ( $I \sim 8$  kA,  $T/2 \sim 175$  ns) and pre-ionization ( $I \sim 20$  A,  $t_{RC} \sim 5$   $\mu$ s) electric currents flowing through the double plasma channel ( $2l_{pl} = 2 \times 18$  cm) were measured by Rogowsky coils. Soft X-ray emission was detected by a fast vacuum X-ray photodiode (XRD).

The examples of pumping currents ( $I \sim 8$  kA,  $T/2 \sim 175$  ns) flowing through the two plasma channels of the double Z-pinch discharge are shown in Fig. 2 (a).



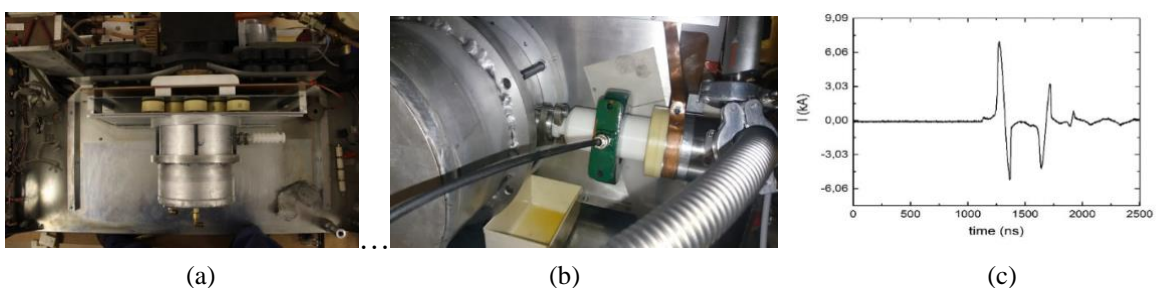
*Fig.2*  
(a) The pumping currents in the two plasma channels. The modeled (b) and experimental (c) laser beams.

Figure 2 also demonstrates the modeled (b) and experimental (c) intensity distributions in the  $\text{Ar}^{+8}$ -laser beam. The relatively low intensity of the laser beam (c) is attributed to the asymmetries and fluctuations of the pumping currents (Fig. 2 (a)) in the two plasma channels.

The computer simulations and experimental results have shown that the low inductance of the double plasma channel provides the pumping currents with shorter amplitudes for more effective pumping of the capillary  $\text{Ar}^{+8}$ -lasers. While the fluctuations and asymmetries of both the pre-ionization and main-pumping (Fig. 2 (a)) currents in the plasma channels impose limits on the stability of the three-electrode Z-pinch and the laser output.

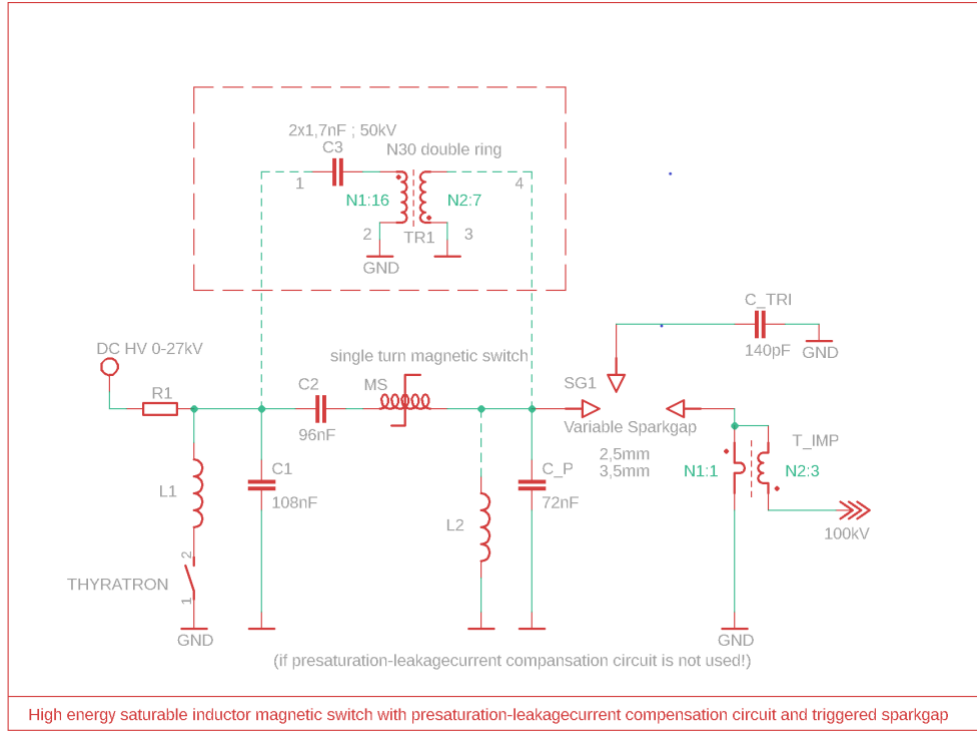
#### 4. Soft X-ray $\text{Ar}^{+8}$ laser using impulse transformer

The  $\text{Ar}^{+8}$  lasers can operate by using the capillary Z-pinch pulses produced by impulse transformers driven by the high-voltage Marx-generator. In the present study, the soft x-ray  $\text{Ar}^{+8}$  laser is pumped by the Marx-less system that uses the 1:4 auto step-up impulse transformer. The energy was stored by a capacitor with the stored energy  $E \sim 100$ J. In the case of 15-25 kV primary-winding voltage, under optimal conditions, we achieved 90-100 kV output pulses with current-amplitude  $\sim 8$  kA and rise-time  $\sim 80$ ns.



*Fig.3*  
The (a) and (b) photos of the pumping system based on the use of impulse transformer. (c) The pumping current.

The experiments with the pumping system based on the use of an impulse transformer showed that the pumping power is not sufficient for the laser operation. Our new  $\sim 3$  times-more-powerful transformer-based system is shown in Fig. 4. The experiments with the new system are in progress.



(a)



(b)

Fig.4

The scheme (a) and photo (b) of our new more powerful pumping system based on the use of impulse transformer.

## 5. Wakefield acceleration of electrons in plasma-waveguides produced by capillary Z-pinches

The waveguide properties of the capillary Z-pinch plasma were obtained from space and frequency-dependent wave equation that combines the attenuated charged particle inertia and the light wave effects in the plasma for the ideal Gaussian laser beam. For a simulation of the temporal and spatial evolution of plasma variables during the capillary discharge, we used our MHD model complemented with atomic data of hydrogen. For a simulation of the wake-field acceleration, we used the particle-in-cell (PIC) model of acceleration of electrons combined with the MHD model. The model can be summarized as follows. Newton's 2nd law for j-th electron with relativistic correction is given by

$$\frac{d}{dt}(m_e \gamma^j \vec{v}_e^j) = \vec{F} \quad (10)$$

where  $m_e$  is the electron rest mass,  $\gamma^j = (1 - \vec{v}_e^{j2} / c^2)^{-1/2}$  is the relativistic factor, and  $\vec{F} = \vec{F}_e + \vec{F}_p$  is the force acting on electron. It is superposition of two most dominant electric and ponderomotive forces:

$$\vec{F} = -e\vec{E} - \frac{e^2 \nabla \vec{E}_L^2}{4m_e \omega_0^2} \quad (11)$$

Here,  $\vec{E} = -\nabla U$  is the electric field caused by charge separation,  $\vec{E}_L$  is the electric field amplitude of laser and  $\omega$  is the central angular frequency of laser pulse. Electric field caused by charge separation can be obtained from Poisson's equation

$$-\nabla^2 U = \rho / \epsilon_0 \quad (12)$$

where  $\rho = \langle Z \rangle en_i - en_e$  is the charge density. In the discrete case of PIC model, the expression in bracket can be written as follows

$$\rho^d = e(N_i - N_e) = e \sum_{j=1}^{N_i} \int_{\Omega} \delta(r - q_i^j) d^3r - e \sum_{k=1}^{N_e} \int_{\Omega} \delta(r - q_e^k) d^3r \quad (18)$$

where  $q_e^j$  and  $q_i^j$  are the positions of j-th electron and ion. Combining these equations, we get the system of equations of density perturbation model that includes the following equations

$$\left( \frac{\partial^2}{\partial t^2} + \omega_{pe}^2 \right) \gamma \delta n_e = \nabla \cdot \left( \frac{e^2 n_{e0}}{4m_e^2 \omega_0^2} \nabla \vec{E}_L^2 \right) - \frac{e}{m_e} \vec{E} \cdot \nabla n_{e0} \quad (13)$$

$$\nabla \cdot \vec{E} = -\frac{e}{\epsilon_0} \delta n_e \quad (14)$$

$$\gamma = \left( 1 + \frac{e^2 \vec{E}_L^2}{2m_e^2 c^2 (\omega_0^2 + f_{ei}^2)} \right)^{1/2} \quad (30)$$

The evolution of the electron density and energy gain during the acceleration was computed by using the PIC model for different wave-guiding regimes, which occur at the propagation time of 0-10 ps (Fig. 5). The studies were conducted for the input peak intensity of  $10^{18} \text{W/cm}^2$ . The peak value of the Z-pinch current pulse, half-cycle duration, and the initial gas pressure were set to 10 kA, 100 ns, and 1.1 mbar, respectively.

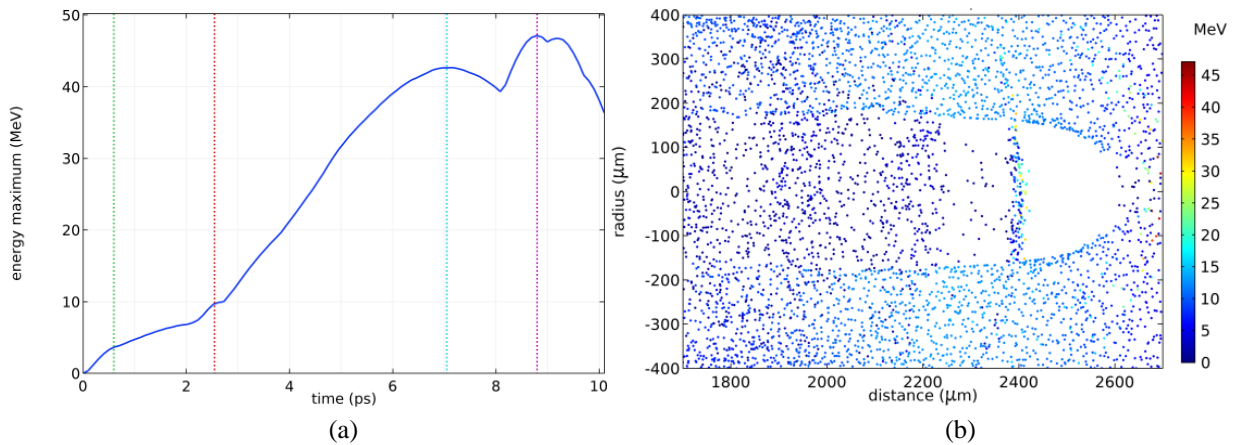


Fig.5

(a) The maximum electron energy vs time. (b) The energy and spatial distribution of electrons at 9 ps.

Simulations demonstrated the repetitive focusing and defocusing patterns with intensity increase at the focal points. The quasi-synchronization of the electron energy maxima with the inflection points

between peaks of the intensity of the guided laser beam was demonstrated. The effect can be used for the optimization of the electron acceleration in plasma waveguides produced by the capillary Z-pinch.

### Summary

The soft x-ray Ar<sup>+8</sup> lasers and wake-field electron accelerators in the low-current capillary Z-pinches have been investigated theoretically and experimentally. The presented studies showed that the low inductance of the double plasma channel provides the pumping currents with shorter amplitudes for more effective pumping of the capillary Ar<sup>+8</sup>-lasers. While the fluctuations and asymmetries of both the pre-ionization and main-pumping currents in the plasma channels impose limits on the stability of the three-electrode Z-pinch and the laser output. The experiments with the low-power pumping system based on the use of an impulse transformer showed that the pumping power is not sufficient for the laser operation. The experiments with our new ~ 3 times-more-powerful transformer-based system are in progress. Our computer simulations of the wake-field electron accelerators in the low-current capillary Z-pinch demonstrated the repetitive focusing and defocusing patterns with intensity increase at the focal points. The synchronization of the electron energy maxima with the inflection points between peaks of the intensity of the guided laser beam was demonstrated. The effect can be used for the optimization of the wake-field electron acceleration in plasma waveguides produced by the capillary Z-pinch.

### Acknowledgements

The project was supported by grant EFOP-3.6.2-16-2017-00005 entitled Ultrafast physical processes in atoms, molecules, nanostructures, and biological systems.

### References

- [1] Y. Sakai, T. Komatsu, I. Song, M. Watanabe, G. H. Kim, and E. Hotta, Review of Scientific Instruments **81**, 013303 (2010).  
<https://doi.org/10.1063/1.3276705>
- [2] C.A. Tan and K.H. Kwek, J. Phys. D: Appl. Phys. **40**, 4787 (2007).  
<https://doi.org/10.1088/0022-3727/40/16/008>
- [3] P. V. Sasorov, N. A. Bobrova, and O. G. Olkhovskaya, The two-temperature equations of magnetic hydrodynamics of the plasma (Keldysh Institute Preprints, 2015).
- [4] A. A. Shapolov, M. Kiss, and S.V. Kukhlevsky, IEEE Trans. Plasma Sci. **46**, 3886 (2018).  
<https://doi.org/10.1109/TPS.2018.2841646>
- [5] T. Hosokai T et al., Opt. Lett. **25**, 10 (2000).  
<https://doi.org/10.1364/OL.25.000010>
- [6] A. Zigler A et al., Appl. Phy. Lett. **113**, 183505 (2018).  
<https://doi.org/10.1063/1.5046400>